Journal of Food and Drug Analysis

Volume 30 | Issue 2 Article 7

2022

Camphorataimide B suppresses the metastasis of human colorectal cancer cell by inhibiting Smad/FAK/Akt axis and promoting degradation of Snail/BMP4 complex

Recommended Citation

Huang, Chi-Chou; Hung, Chia-Hung; Lee, Yi-Ju; Tseng, Tsui-Hwa; Lee, Yean-Jang; Kao, Shao-Hsuan; and Wang, Chau-Jong (2022) "Camphorataimide B suppresses the metastasis of human colorectal cancer cell by inhibiting Smad/FAK/Akt axis and promoting degradation of Snail/BMP4 complex," *Journal of Food and Drug Analysis*: Vol. 30 : Iss. 2 , Article 7.
Available at: https://doi.org/10.38212/2224-6614.3405

This Original Article is brought to you for free and open access by Journal of Food and Drug Analysis. It has been accepted for inclusion in Journal of Food and Drug Analysis by an authorized editor of Journal of Food and Drug Analysis.

ORIGINAL ARTICLE

Camphorataimide B suppresses the metastasis of human colorectal cancer cell by inhibiting Smad/FAK/Akt axis and promoting degradation of Snail/BMP4 complex

Chi-Chou Huang [a,b,1], Chia-Hung Hung [c,1], Yi-Ju Lee [d,e], Tsui-Hwa Tseng [f], Yean-Jang Lee [g], Shao-Hsuan Kao [c,h,**], Chau-Jong Wang [c,h,i,*]

[a] Department of Colorectal Surgery, Chung Shan Medical University Hospital, Taichung, Taiwan
[b] School of Medicine, Chung Shan Medical University, Taichung, Taiwan
[c] Institute of Medicine, College of Medicine, Chung Shan Medical University, Taichung, Taiwan
[d] Department of Pathology, Chung Shan Medical University Hospital, Taichung, Taiwan
[e] Department of Pathology, School of Medicine, Chung Shan Medical University, Taichung, Taiwan
[f] Department of Medical Chemistry, Chung Shan Medical University, Taichung, Taiwan
[g] Department of Chemistry, National Changhua University of Education, Changhua, Taiwan
[h] Department of Medical Research, Chung Shan Medical University Hospital, Taichung, Taiwan
[i] Department of Health Diet and Industry Management, Chung Shan Medical University, Taichung, Taiwan

Abstract

Camphorataimide B (CamB) has anticancer activities against several tumors. Here, we aimed to investigate the mechanism(s) by which CamB inhibits metastasis of colorectal cancer (CRC) cells. Low-dose CamB did not affect the cell viability and cell cycle progression of CRC cells, but significantly inhibited the metastatic potentials of CRC cells. Mechanically, CamB reduced the protein and mRNA expression of BMP4, and inhibited Smad and FAK/Src/Akt signaling. CamB also decreased Snail levels by promoting its degradation via proteasome and thereafter reduced Snail-mediated BMP4 transcription. Moreover, CamB considerably inhibited the *in vivo* metastasis of DLD-1 cells in xenograft mice.

Keywords: Bone morphogenetic protein 4, Camphorataimide-B, Colorectal cancer, FAK, Snail

1. Introduction

Colorectal cancer (CRC) is a leading life-threatening malignancy worldwide, and the morbidity and mortality of CRC have increased in the past decade [1]. CRC originates from dysplastic adenomatous polyps and gradually transforms into invasive carcinoma because of genetic modifications that reinforce colorectal epithelial cell growth and suppress colorectal epithelial cell apoptosis [2]. Today, the combination of chemotherapy and surgery has been widely used in patients with CRC; however, the high recurrence and distant metastasis of CRC cells still lead to the poor survival of patients

Abbreviations: CamB, Camphorataimide B; CRC, Colorectal cancer; qPCR, Quantitative real-time polymerase chain reaction; BMP4, Snail/bone morphogenetic protein 4; FAK, Focal adhesion kinase; DMSO, Dimethyl Sulfoxide - Polar Organic Reagent; MTT, 3-(4,5-dimethylthiazol-2-yl)-2,5-diphenyltetrazolium bromide; PI, propidium iodide; FBS, Fetal bovine serum; HRP, Horse radish peroxidase; H&E, Hematoxylin and eosin; TGF, Transforming growth factor,

Received 28 November 2021; revised 20 February 2022; accepted 24 February 2022.
Available online 15 June 2022

* Corresponding author at: Institute of Medicine, College of Medicine, Chung Shan Medical University, No.110, Sec. 1, Jianguo N. Rd., Taichung, 402, Taiwan. Fax: +886-4-2324-8167.
** Corresponding author at: Institute of Medicine, College of Medicine, Chung Shan Medical University, No.110, Sec. 1, Jianguo N. Rd., Taichung, 402, Taiwan. Fax: +886-4-2324-8167.
E-mail addresses: kaosh@csmu.edu.tw (S-H. Kao), wcj@csmu.edu.tw (C-J. Wang).
[1] These authors contributed equally.

https://doi.org/10.38212/2224-6614.3405

with CRC with late-stage progression [1]. Cell adhesion, cell motility, and invasive capability play a central role in CRC metastasis [3]. Therefore, the inhibition of CRC metastasis has been recognized as a promising approach to improve CRC treatments and increase the survival rate of patients with CRC.

The identification of phytochemicals with anticancer activity has been an important strategy to develop novel therapeutic adjuvants for cancer treatments and even novel anticancer drugs. Over time, some natural compounds have been demonstrated to have *in vitro* or *in vivo* chemopreventive and anticancer activities [4–6]. *Antrodia camphorata* is a medicinal fungus (*Ganoderma* species) of the Polyporaceae family that commonly grows in camphor tree in Taiwan. In the past two decades, the various biological functions of *A. camphorata* mycelium, including anti-inflammatory, anti-oxidative, and anticancer activities, have been reported [7]. Camphorataimide B (CamB), a derivative isolated from *A. camphorata* mycelium, has been reported to have anticancer effect against breast cancer cells [8].

Here, we aimed to explored the anti-metastatic effects of CamB on CRC cells and the underlying mechanism. Metastatic potentials were evaluated by using transmigration, invasion assays, and xenograft mouse model. Molecular mechanisms were demonstrated using Western blot, quantitative real-time polymerase chain reaction (qPCR), chromatin immunoprecipitation, and reporter assay. Our findings reveal that CamB can inhibit the metastatic potentials of CRC cells through the suppression of the Smad/FAK/Akt axis and the promoted degradation of Snail/bone morphogenetic protein 4 (BMP4) complex via promoting ubiquitin-mediated proteasome degradation.

2. Materials and methods

2.1. Chemicals, reagents, and antibodies

CamB was synthesized from succinic anhydride as previously described (Cheng et al., 2008). Crystal violet, 2-propanol, 3-(4,5-dimethylthiazol-2-yl)-2,5-diphenyltetrazolium bromide (MTT), 1-butanol, dimethyl sulfoxide (DMSO), phosphate-buffered saline (PBS), sodium chloride, sodium dodecyl sulfate (SDS), Tris-HCl, type I collagen, and trypsin/EDTA were purchased from Sigma-Aldrich. Antibodies against BMP4, α-actinin, Smad1/5/9, Smad4, Lamin A/C, talin, tensin 2, α-actinin, vinculin, focal adhesion kinase (FAK), phospho-FAK (pY397-FAK), Src, phospho-Src (pY416-Src), p130Cas, AKT, phospho-AKT (pS473-AKT), RhoA, GTP-RhoA, Cdc42, GTP-Cdc42, Rac1, GTP-Rac1, paxillin, phospho-paxillin (pY31-Paxillin, pY118-Paxillin, pY181-Paxillin), Snail, β-actin, and tubulin, as well as peroxidase-conjugated antibodies against mouse or rabbit IgG, were obtained from Santa Cruz Biotechnology, Inc. or Abcam.

2.2. Cell culture

Human colon cancer lines DLD-1, SW480, and SW620 were purchased from BCRC (Hsinchu, Taiwan), cultured in RPMI-1640 and L-15 mediums supplemented with 10% fetal bovine serum (FBS; Biological Industries, Cromwell, CT, USA), and incubated at 37 °C with 5% CO_2. The cells were cultured until 80% confluency and then incubated with the indicated concentrations of CamB for 24 h. The treated cells were harvested, washed with PBS, and then used for subsequent analyses. DMSO (0.1%) treatment was used as the control (Ctrl, or 0 μM).

2.3. Cell viability assay

Cell viability was determined using MTT assay as previously described [9]. Briefly, the cells were treated with CamB at serial concentrations for indicated times, and then incubated with MTT solution. After adding isopropanol to solubilize the formed formazan, the absorbance of the solution at 563 nm was measured using a spectrophotometer. The percentage of viable cells was estimated by comparing with control.

2.4. Cell cycle distribution and cellular apoptosis analyses

Cell cycle distribution and cellular apoptosis were determined by flow cytometry. The cells were synchronized at G_0 by 16-h serum-free starvation, then incubated with the indicated concentrations of CamB for 24 h, trypsinized for detachment, and collected by centrifugation. The collected cells were fixed with 70% ethanol, washed with PBS, incubated with propidium iodide (PI) alone (cell cycle distribution) or with PI and Annexin V (cellular apoptosis) in the dark for 30 min, and then analyzed using a flow cytometer equipped with CellQuest Pro software.

2.5. Cell migration and invasion assays

Cells were pretreated with CamB for 24 h, harvested by trypsinization, and then seeded on 24-well cell culture inserts (8 μm pore size, Millipore). FBS

(20%) placed in the lower compartment of the plate was used as the chemoattractant. After 12 h of incubation, the cells that migrated to the lower surface of the insert were fixed with paraformaldehyde and stained with Giemsa reagent (Sigma-Aldrich). The stained cells were photographed, and the total cell number from five random fields was counted using light microscopy. For the invasion assay, 100 μL of Matrigel (20 × dilution in PBS) was added into the culture inserts and then air-dried prior to cell seeding as described above.

2.6. Cell adhesion assay

Cells were incubated with the indicated concentrations of CamB for 24 h, transferred into 12-well Matrigel-coated plates at 10^5 cells/well, and then incubated at 37 °C for 16 h. After incubation, non-adherent cells were removed by washing with PBS, and the attached cells were photographed and quantitated.

2.7. Clonogenic assay

Cells were suspended in agarose medium containing 0.3% agarose, 10% FBS, and the indicated concentrations of CamB; seeded onto a 6-well plate, which was pre-coated with a layer of solidified 0.6% agarose; and then incubated at 37 °C for 1 week. At the end of incubation, the cell colonies were fixed with methanol/acetic acid (3:1), stained with crystal violet, ant then photographed using a Nikon Eclipse TE2000-U microscope equipped with a Nikon DXM1200 digital camera. The colonies with size ≥0.1 mm were counted for quantitation.

2.8. Immunofluorescence staining

Cells were fixed by 4% ice-cold formaldehyde, reacted with blocking buffer containing 0.5% Triton X-100 for 1 h at 25 °C, and incubated with primary antibodies for 16 h at 4 °C. The cells were washed with PBS, and the bound primary antibodies were detected using Alexa Fluor-labeled secondary antibody (Jackson ImmunoResearch Laboratories, West Grove, PA, USA). Alexa Fluor-conjugated phalloidin (Cell Signaling) was used for the detection of polymerized F-actin microfilaments. Fluorescence image was acquired using a laser scanning confocal microscope system (Zeiss 510-Meta, Zeiss, Oberkochen, Germany).

2.9. Western blot and small GTPase activity assessment

Western blot was conducted as previously described [10]. Briefly, cells were lysed in Tris lysis buffer containing protease and phosphatase inhibitor cocktail (Sigma-Aldrich). Then, the resulting crude proteins were separated by SDS-polyacrylamide gel electrophoresis, transferred to polyvinylidene difluoride membrane (Immobilon, Merck), and then reacted with the primary antibodies following with the secondary antibodies. The bound antibodies was detected using enhanced chemiluminescence reagent (SuperSignal West Dura HRP Detection Kit; Pierce Biotechnology, Rockford, IL, USA) an image analysis system (Fujifilm, Tokyo, Japan).

Small GTPase activity was assessed by GTPase affinity precipitation as previously described [11]. Briefly, cells were lysed in MLB buffer (Millipore, Bedford, MA, USA), and the resulting crude protein were reacted with Rac/Cdc42-binding domain and Rho protein-binding domain agarose conjugate beads. The reacted beads were collected and washed with MLB buffer, and the bound proteins were acquired by boiling the beads with SDS sample buffer and analyzed by Western blot.

2.10. Co-immunoprecipitation assay

Cells were lysed with RIPA buffer containing protease and phosphatase inhibitor cocktail for crude protein extraction. The extracted proteins were pre-cleared with 50 μL of a 50% slurry of protein G-Sepharose beads 4B (GE Healthcare) for 60 min at 4 °C and then incubated with 2 μg of primary antibody or nonspecific IgG (negative control) for 16 h at 4 °C. The protein–antibody complex was collected using recombinant protein G-Sepharose 4B beads and subjected to Western blot analysis.

2.11. RT-PCR and qPCR

Gene expression was assessed by RT-PCR and qPCR as previously described [4]. Briefly, total RNA was isolated from individual samples using TRIzol reagent (Invitrogen, Carlsbad, CA, USA). The purified RNA was used as a template to generate first-strand cDNA using a GoScript reverse transcription kit (Promega, Madison, WI, USA).

2.12. Chromatin immunoprecipitation analysis

Chromatin immunoprecipitation analysis was performed as previously described [12]. The purified, immunoprecipitated DNA was analyzed by RT-PCR and visualized by ethidium bromide staining after gel electrophoresis.

2.13. Reporter assay for transcriptional activity

Cells were transfected with BMP4 promoter-luciferase vectors using Tuberfast transfection reagents for 24 h and then incubated with CamB (10, 20, or 30 μM) for 24 h. The treated cells were washed with PBS and lysed with 50 μL of passive lysis buffer. The resulting lysates were transferred to 96-well plates and incubated with luciferin substrate. Luciferase activity and β-gal enzyme activity were determined using a luciferase assay kit and a microplate reader, respectively, according to the manufacturer's instructions. Relative luciferase activity was presented as the ratio of the fluorescence units of BMP4 reporter plasmid-transfected cells to the fluorescence units of pGL3-Basic-transfected cells.

2.14. Transient Snail overexpression

DLD-1 cells were seeded at 2×10^5 cells/mL in complete medium, cultured until 90% confluency, and transfected with control vector pcDNA3.1 or pCMV-Tag2B-Snail (a gift from Dr. Li-Sung Hsu, Institute of Medicine, Chung Shan Medical University) using T-Pro non-liposomal transfection reagent (T-Pro Biotechnology, Taipei City, Taiwan) according to the manufacturer's instruction for Snail overexpression.

2.15. Xenograft mouse model

Four-week-old male Balb/c nude mice were obtained from the National Laboratory Animal Center of Taiwan (Taipei City, Taiwan) and maintained under the supervision of the Institutional Animal Care and Use Committee at Chung Shan Medical University. All animal experiments were performed under specific pathogen-free conditions in accordance with the approved protocol and institutional guidelines. The metastatic human colon cancer cell line DLD-1 was transduced with a lentivirus expressing firefly luciferase to produce luciferase-expressing DLD-1 (Luc-DLD-1). Luc-DLD-1 cells (2×10^6) were injected into the peritoneum of nude mice by surgical procedure for the assessment of abdominal. In parallel, Luc-DLD-1 cells were also injected into the spleen of nude mice for the specific assessment of liver metastases as previously described [13]. The mice were randomly divided into four groups (5 mice/group) on day 6 after the injection of Luc-DLD-1 and orally administrated with 10 or 20 mg/kg CamB every 3 days for 35 days for the metastasis assessments. The mice for *in vivo* tumor growth assessment were anesthetized and received an intraperitoneal injection of luciferin (150 mg/kg body weight prepared in PBS). The resulting bioluminescence images were captured using an IVIS-200 imaging system (Xenogen, Alameda, CA, USA) and processed using Living Image software (Xenogen) through the region-of-interest analysis of the total photons per second. At the end of image acquirement, the mice were sacrificed to evaluate the metastasis of cancer cells by determining organ weights and immunohistochemical (IHC) staining.

2.16. Histopathological examination and IHC staining

The tissues were collected, cut into small pieces, fixed with 10% buffered neutral formaldehyde, and embedded in paraffin. Then, the embedded tissues were cut into sections with a thickness of 3–5 μm. The sections for histopathological examination were stained with hematoxylin and eosin (H&E). Histopathological properties were examined by light microscopy at 400 × magnification. The sections for IHC staining were blocked with BSA, reacted with antibodies against human BMP4 and Snail, and washed with PBS. The washed sections were incubated with HRP-conjugated anti-IgG antibodies and reacted with the substrate–chromogen reagent. Images were acquired through a charge-coupled device camera and analyzed using an image analysis system (Fujifilm).

2.17. Statistical analysis

The data from three independent experiments were presented as the mean ± standard deviation (SD) except where indicated. Student's *t*-test was used to analyze the significance of difference. Results with $p < 0.05$ were considered statistically significant.

3. Results

3.1. Effects of CamB on human CRC cells

The structure of CamB is shown in Fig. 1A. The effects of CamB on the cell viability and morphology

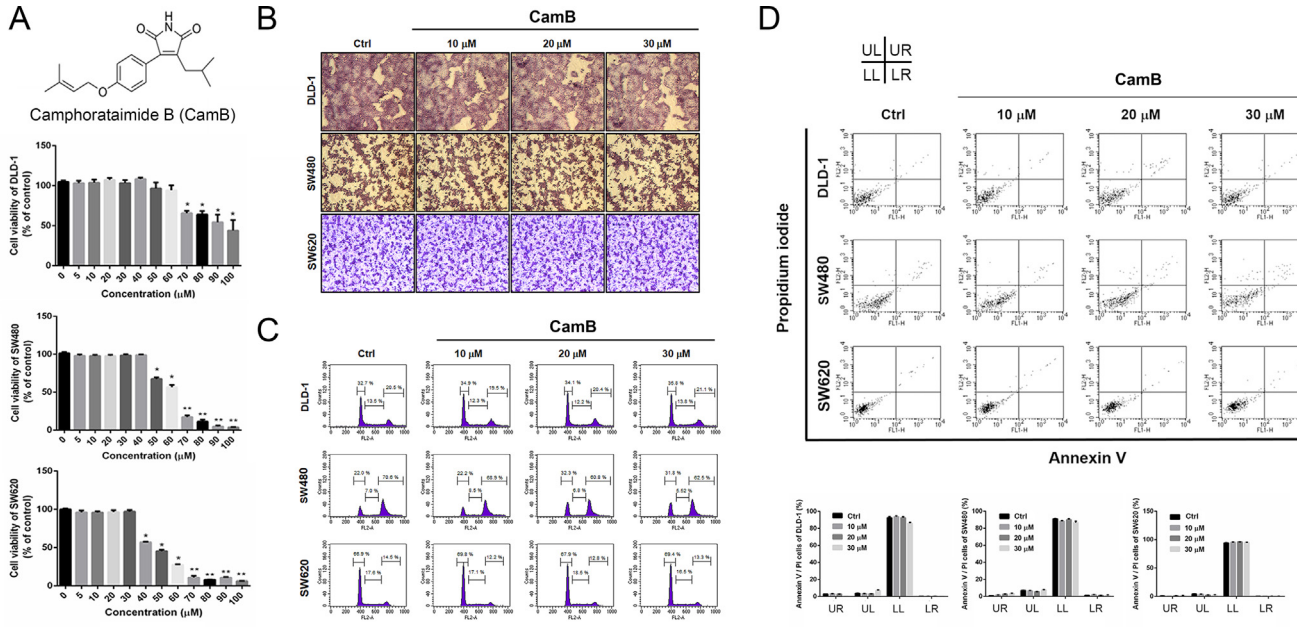

*Fig. 1. Effects of CamB on cell viability, cell morphology, cell cycle progression, and cellular apoptosis of CRC cells. (A) Chemical structure of CamB and cell viability of DLD-1, SW480, and SW620 cells treated with serial concentrations (0–100 μM) of CamB for 24 h. (B) H&E staining for monitoring the cell morphology of CRC cells treated with CamB for 24 h. (C) Cell cycle distribution analysis by PI staining and flow cytometry. (D) Cell apoptosis analysis of cells treated with indicated CamB concentrations for 24 h using PI/Annexin V staining and flow cytometry. Quantitative results are presented as mean ± SD. * and **, $p < 0.01$ and $p < 0.001$ compared with control, respectively.*

of human CRC cell lines DLD-1, SW480, and SW620 were first explored. As shown in Fig. 1A, the cell viability of these cells was reduced by high-doses CamB (50–100 μM), but not affected by low-doses CamB (≤30 μM) compared with DMSO control. Next, we focused on the anti-tumorigenic activity of low-doses CamB (10–30 μM). Low-doses CamB neither influenced the cell morphology and cell cycle progression nor induced the cellular apoptosis of tested CRC cells (Fig. 1B–D).

3.2. CamB attenuates migration and invasion of CRC cells and downregulates cellular F-actin expression

Next, we explored the effects of CamB on metastatic potentials of CRC cells. As shown in Fig. 2A, the low-doses CamB (20 and 30 μM) significantly attenuated the migration and invasion of the tested CRC cells ($p < 0.05$ compared with control). In addition, the low-doses CamB also reduced the cell adhesion and colony formation ability of the tested CRC cells (Fig. 2B and C, for 20 and 30 μM, $p < 0.05$ compared with control). Then, we examined the effects of CamB on the cytoskeleton organization that was closely related to cell adhesion and cell motility. The results showed that 30 μM CamB disrupted normal cytoskeletal actin organization compared with control (Fig. 2D). Together, these findings reveal that low-doses CamB can reduce the metastatic potentials of CRC cells.

3.3. Downregulated BMP4 expression and Samd/FAK signaling are associated with the inhibited metastatic potentials of CRC cells in response to CamB

Multiple mediators produced by cancer cells are involved in the metastatic dissemination of tumors. Therefore, we investigated whether CamB alters the production of metastasis-associated mediators by CRC cells. By cytokine array analysis, we observed that the production of angiogenin, CXCL13/B lymphocyte chemoattractant, BMP4, ciliary neurotrophic factor, CCL11/eotaxin-3, and insulin-like growth factor binding protein 2 by DLD-1 cells were significantly decreased in response to CamB treatment ($p < 0.05$ compared with control, Fig. 3A and B). On the contrary, CamB increased the production of granulocyte-macrophage colony-stimulating factor, macrophage colony-stimulating factor, and CXCL7/neutrophil activating peptide 2 by DLD-1 cells ($p < 0.05$ compared with control). Among these mediators, the production of BMP4 was greatly reduced; therefore, we further investigated the role of BMP4, a member of the transforming growth factor beta (TGF-β) superfamily, in the CamB-inhibited metastatic power by exploring the

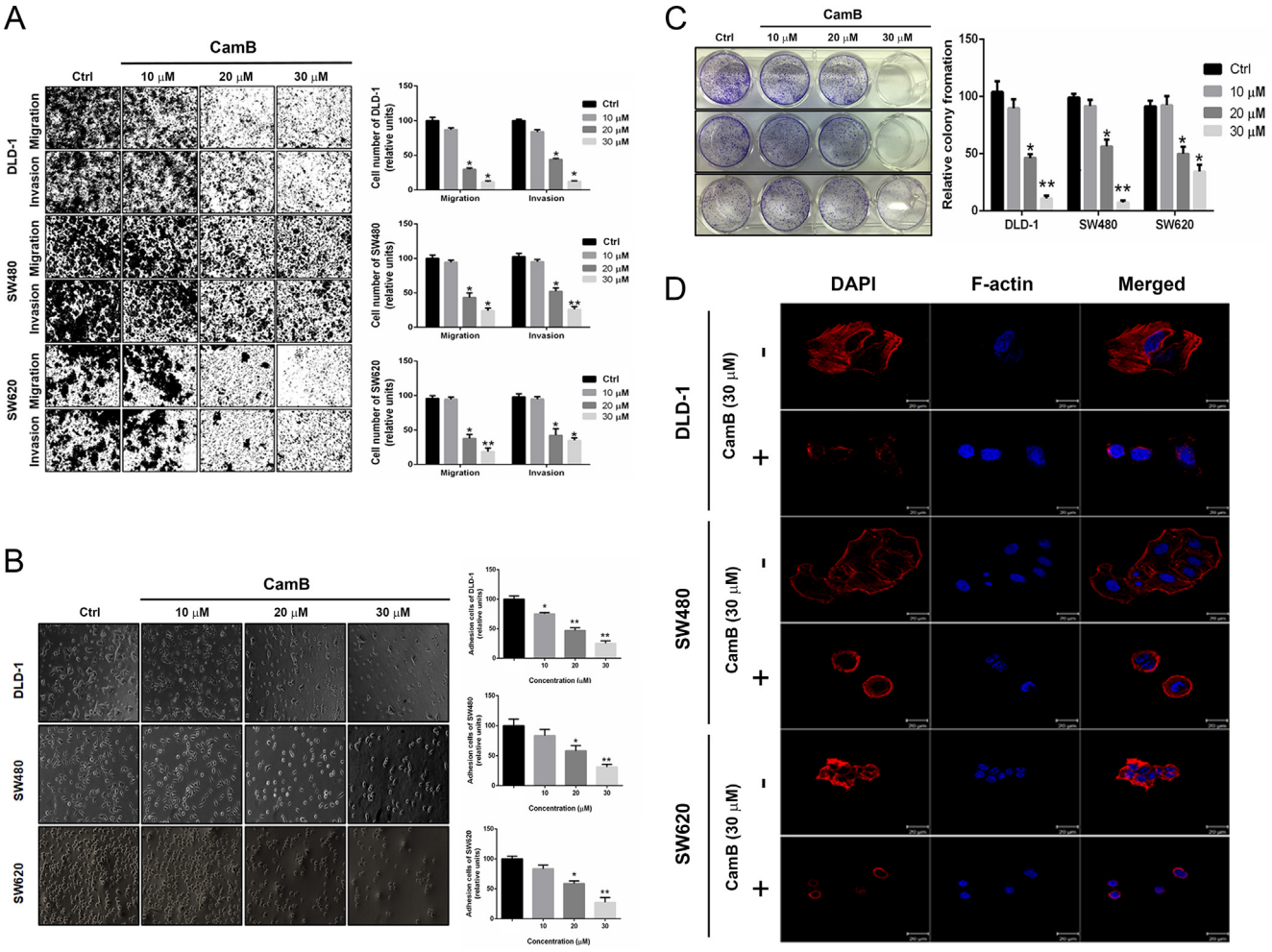

*Fig. 2. Low-doses CamB inhibit migration, invasion, and adhesion of CRC cells and disrupt cytoskeleton organization. Cells were treated with CamB at indicated concentrations for 24 h, and then subjected to (A) transmigration and invasion assay, (B) cell adhesion assay, (C) colony formation assay, and (D) cytoskeleton structure assay using immunofluorescence staining and confocal microscopy (200×). F-actin is shown as red. Nuclei are shown as blue by DAPI staining. Quantitative results are presented as mean ± SD. * and **, $p < 0.01$ and $p < 0.001$ compared with control, respectively.*

effects of CamB on important signaling components associated with cancer metastasis. Our results showed that CamB dose-dependently reduced the protein and mRNA expression of BMP4 (Fig. 3C and D), inhibited the BMP4 canonical Smad signaling, and suppressed focal adhesion cascade, including FAK/Src/paxillin axis (Fig. 3E–H), and small GTPase Rho/Cdc42/Rac activation (Fig. 3I and J) in DLD-1 and SW480 cells. Collectively, these findings reveal that CamB can regulate the production of cytokines and signaling pathways that were strongly associated with the metastatic power of CRC cells.

3.4. BMP4 restores the metastatic power of CRC cells and the Smad/FAK signaling reduced by CamB

Next, we analyzed the effects of BMP4 on the metastatic potentials of DLD-1 and SW480 cells to further explore the involvement of BMP4 in the inhibition of metastatic potential by CamB. As shown in Fig. 4A and B, BMP4 treatments promoted the cell adhesion and colony formation capabilities of DLD-1 and SW480 cells ($p < 0.05$ compared with control). Similarly, the migratory and invasive capacities of both cell lines were also enhanced by BMP4 treatment (Fig. 4C and D, $p < 0.05$ compared with control). Likewise, BMP4 significantly restored the metastatic potentials that were reduced by CamB (Fig. 4E–H, $p < 0.05$ compared with CamB treatment alone). We also observed by confocal microscopy analysis that BMP4 clearly induced the spread of cytoskeleton and resulted in the expansion of cell shape, which were inhibited by CamB (Fig. 4I). Then, we investigated the effects of BMP4 on CamB-mediated Smad and FAK cascades in DLD-1 and SW480 cells. Our results showed that BMP4 alone slightly induced the phosphorylation of Smad1/5/9,

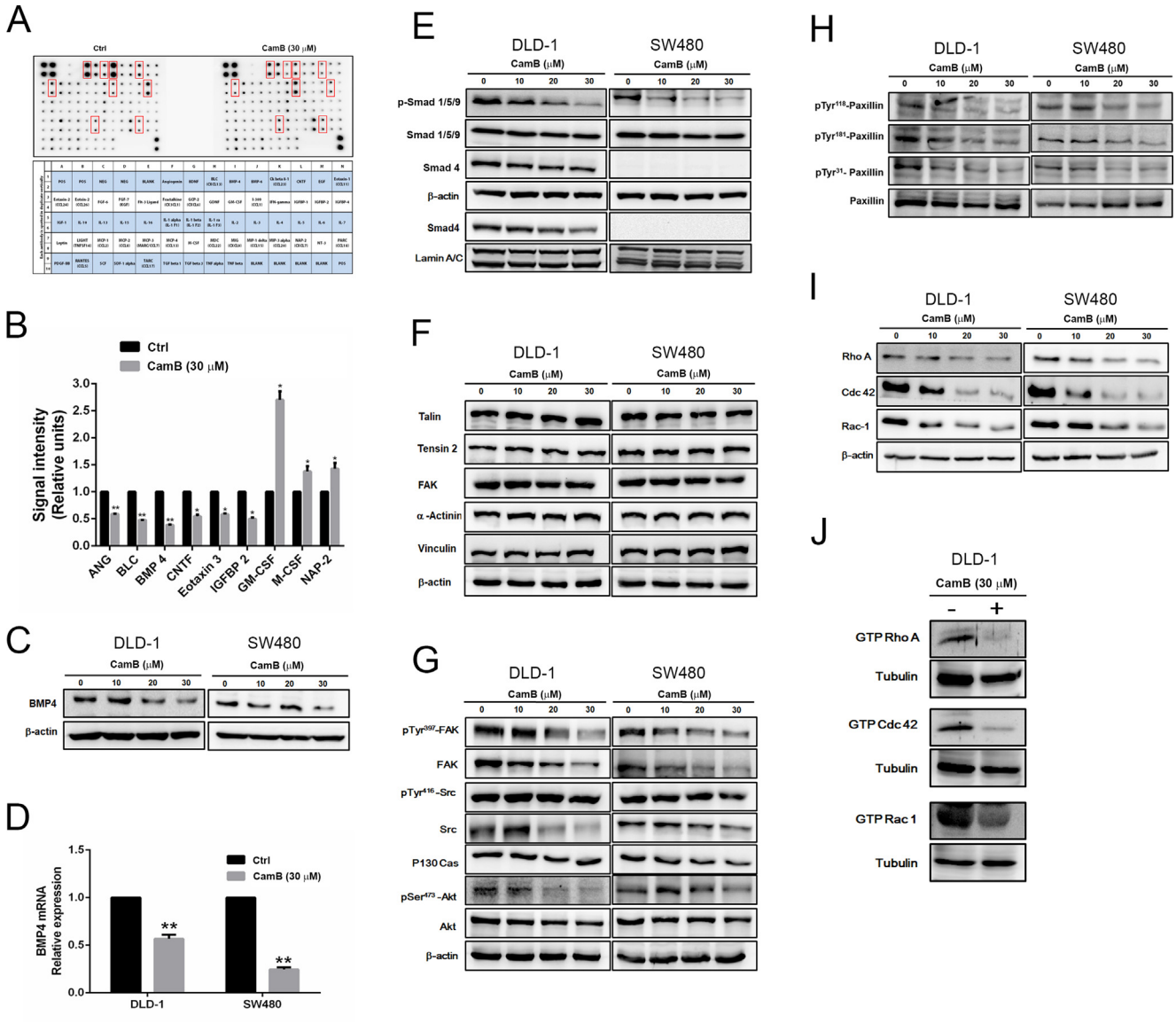

*Fig. 3. CamB downregulates BMP4 and inhibited FAK signaling and Rho A small GTPase activation in CRC cells. (A–D) Cells were treated with 30 μM CamB for 24 h, washed with PBS and incubated with serum-free medium for 24 h, then the culture medium was collected for human cytokine array, and the cells were harvested for Western blot and qPCR analysis. (A) Representative array image for cytokine production by DLD-1 cells. (B) Quantitative results of array analysis; (C, D) Protein and mRNA expression of BMP4 in DLD-1 cells. (E–J) Cells were treated with 30 μM CamB for 24 h, and then lysed for Western blot and GTPase activity assay. (E) Phosphorylation and expression of Smads in total and nucleus fraction; (F) Expression of integrin-associated signaling components; (G) Activation of FAK-associated signaling components; (H) Phosphorylation of paxillin; (I) Protein level of small GTPases; (J) GTPase affinity precipitation followed Western blot. β-actin and tubulin were used as the internal controls. Quantitative results are presented as mean ± SD. * and **, $p < 0.01$ and $p < 0.001$ compared with the control, respectively.*

FAK(Y937), Src(Y416), and paxillin (Y118/Y181/Y31), as well as restored the phosphorylation of these Smad/FAK signaling components inhibited by CamB (Fig. 4J and K). Simialrly, BMP4 also restored the protein expression of RhoA, Cdc42, and Rac1 inhibited by CamB in DLD-1 and SW480 cells (Fig. 4). Collectively, these findings indicate that BMP4 can restore the metastatic power of CRC cells and the Smad/FAK and Rho/Cdc42/Rac signaling cascade inhibited by CamB in CRC cells. Thus, BMP4 plays an important role in the inhibitory effect of CamB on the metastatic power of CRC cells.

3.5. CamB downregulates BMP4 expression by promoting ubiquitin-mediated Snail protein degradation

Epithelial–mesenchymal transition (EMT) inducer Snail is a transcription factor that plays pivotal roles in reinforcing the metastatic potential

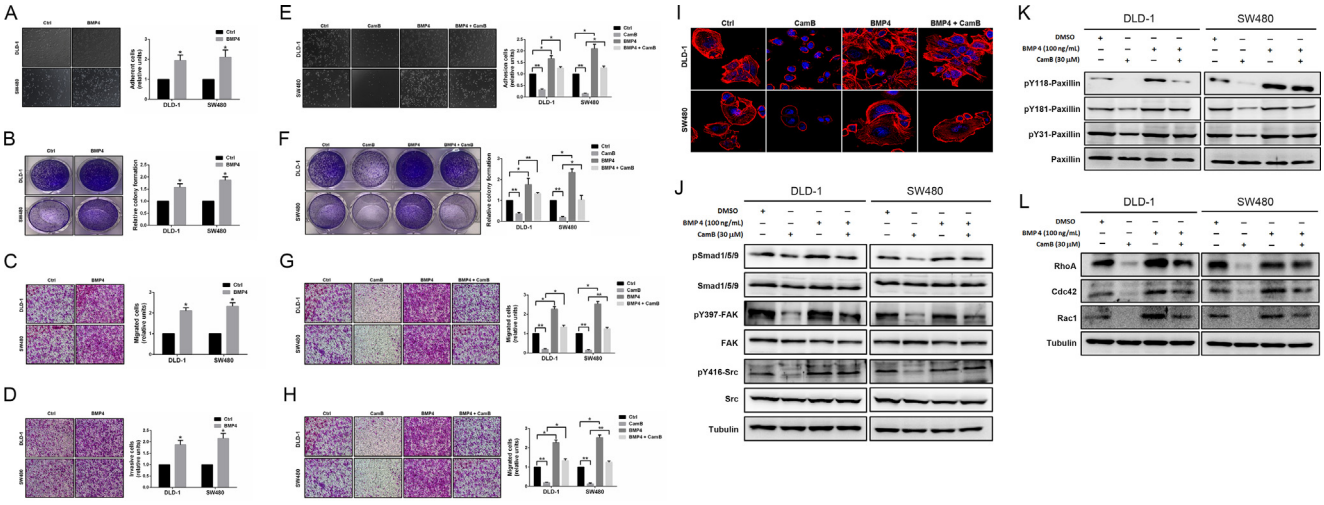

Fig. 4. ***Involvement of BMP4 in CamB-inhibited metastatic potential and signaling cascade in colon cancer cells.*** *(A–D) Cells were treated with recombinant BMP4 (50 ng/mL) for 24 h and then subjected to (A) Cell adhesion assay, (B) Colony formation assay, (C) Migration assay, and (D) Invasion assay. (E–L) Cells were pretreated without or with recombinant BMP4 (50 ng/mL) for 2 h, then treated with 30 μM CamB for 24 h, and subjected to (E) Cell adhesion assay; (F) Colony formation assay; (G) Migration assay; (H) Invasion assay; (I) Immunofluorescence assay for F-actin (red); and (J–L) Western blot for the phosphorylation and expression of (J) Smad, FAK, and Src; (K) paxillin; and (L) Rho small GTPases. Nuclei (blue) were detected by DAPI staining. Tubulin was used as the internal control. Quantitative results are presented as mean ± SD. * and **, $p < 0.01$ and $p < 0.001$ compared with the control, respectively.*

of CRC cells through the regulation of cell motility, invasiveness, and cell adhesion [9]. Next, we explored the mechanism by which CamB inhibited BMP4 transcription in CRC cells and the link between Snail and BMP4. As shown in Fig. 5A and B, CamB inhibited Snail protein expression and reduced Snail in the nucleus of DLD-1 and SW480 cells. To further explore whether Snail regulate BMP4 transcription, BMP4 promoter region (Gene ID: LOC109433677) were used for searching putative Snail binding motif, and the results showed that the proximal promoter of the BMP4 gene included a putative E-box binding motif CANNTG for Snail (data not shown). Then, we demonstrated by chromatin immunoprecipitation and reporter assay that Snail directly bound to the putative E-box on BMP4 promoter and CamB was able to inhibit the transcriptional activity induced by BMP4 promoter (Fig. 5C and D). We also overexpressed Snail in DLD-1 and SW480 cells by transfecting Snail-expressing vectors and similarly observed that CamB inhibited the binding of Snail to BMP4 promoter (Fig. 5E). Further investigation showed that CamB did not alter mRNA expression of Snail (Fig. 5F), and pretreatment of cycloheximide, a protein synthesis inhibitor, promoted the downregulation of Snail in response to CamB (Fig. 5G). Meanwhile, pretreatment of MG132, a proteasome inhibitor, restored the downregulation and ubiquitination of Snail in response to CamB (Fig. 5H and I). Collectively, these results indicate that Snail plays an important role in BMP4 expression, and CamB promotes the ubiquitin-mediated protein degradation of Snail and therefore inhibits the transcription of BMP4.

3.6. CamB inhibits the in vivo metastasis of DLD-1 cells and downregulates BMP4 and Snail expression in DLD-1-derived tumor

We demonstrated the *in vivo* effect of CamB on the metastasis of CRC cells using a xenograft mouse model. As shown in Fig. 6A, the oral administration of CamB (10 and 20 mg/kg) clearly reduced the metastasis of Luc-DLD-1 cells in the liver and abdomen using an *in vivo* imaging system (Fig. 6A). We observed that CamB alone did not influence the phenotype of spleen, liver, and colon tissues compared with the control group. Meanwhile, CamB clearly reduced the Luc-DLD-1 cells that grew in the spleen and colon and those that metastasized to the liver of xenograft mice (Fig. 6B and C). Further IHC staining analysis showed that the Luc-DLD-1 cells that transferred to the liver highly expressed BMP4 and Snail, and CamB administration remarkably reduced the BMP4 and Snail expression of Luc-DLD-1 cells in the liver (Fig. 6D and E). Taken together, these observations reveal that CamB administration inhibits the *in vivo* metastasis of DLD-1 colon cancer cells into the liver, colon, and spleen, and this inhibition is associated with the decreased expression of BMP4 and Snail.

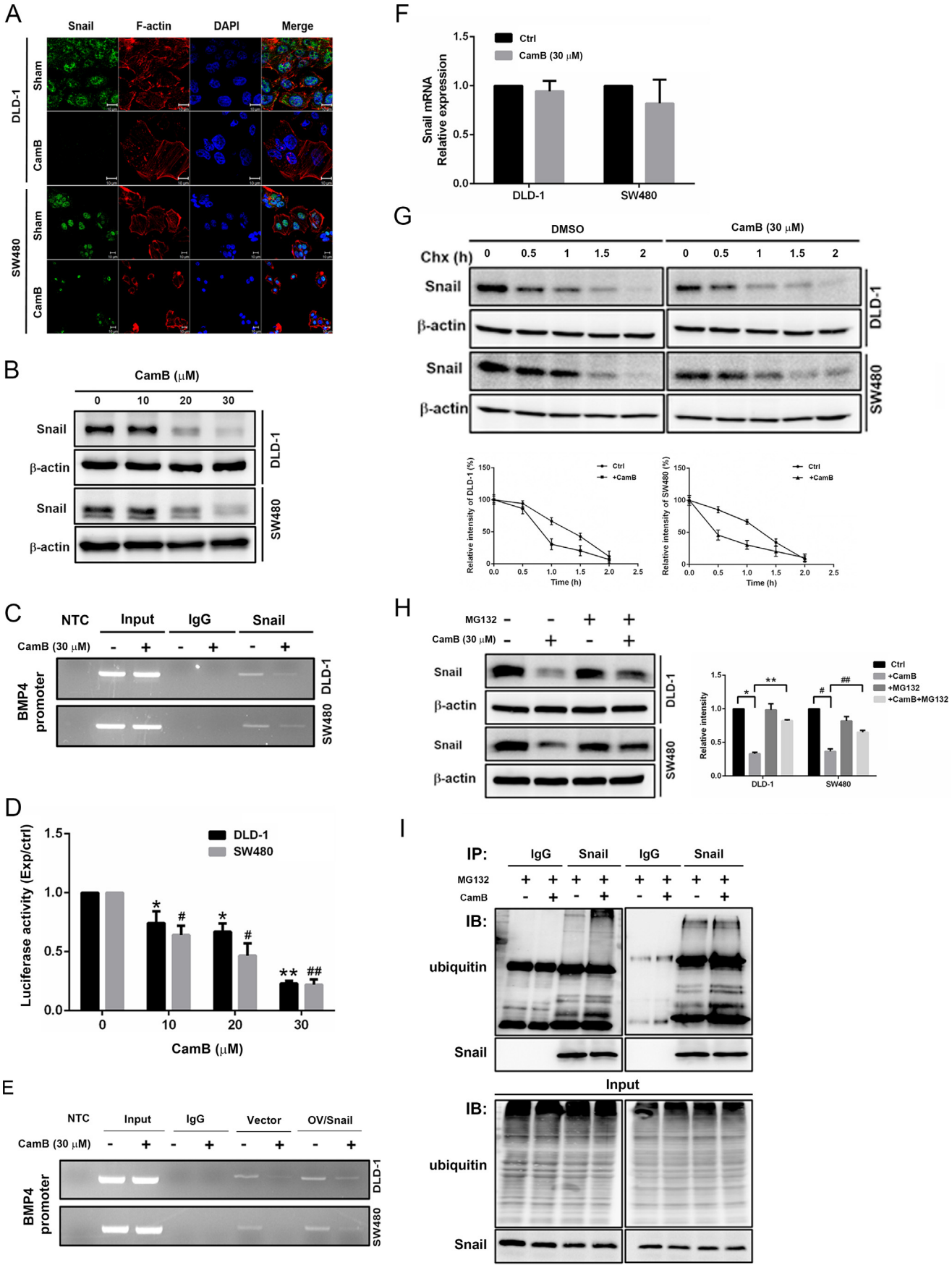
A
Snail
F-actin
DAPI
Merge
DLD-1
Sham
CamB
SW480
Sham
CamB
B
CamB (μM)
0
10
20
30
Snail
β-actin
Snail
β-actin
DLD-1
SW480
C
NTC
Input
IgG
Snail
CamB (30 μM)
BMP4 promoter
DLD-1
SW480
D
DLD-1
SW480
Luciferase activity (Exp/ctrl)
CamB (μM)
E
NTC
Input
IgG
Vector
OV/Snail
CamB (30 μM)
BMP4 promoter
DLD-1
SW480
F
Ctrl
CamB (30 μM)
Snail mRNA Relative expression
DLD-1
SW480
G
DMSO
CamB (30 μM)
Chx (h)
0
0.5
1
1.5
2
Snail
β-actin
DLD-1
SW480
Ctrl
+CamB
Relative intensity of DLD-1 (%)
Relative intensity of SW480 (%)
Time (h)
H
MG132
CamB (30 μM)
Snail
β-actin
DLD-1
SW480
Ctrl
+CamB
+MG132
+CamB+MG132
Relative intensity
I
IP:
IgG
Snail
MG132
CamB
IB:
ubiquitin
Snail
Input
IB:
ubiquitin
Snail

*Fig. 5. CamB reduced Snail protein stability and its binding to the BMP4 promoter via promoting ubiquitin-proteasome degradation in CRC cells. (A) Cells were treated with 30 μM CamB for 24 h, and the protein levels of Snail (green) and F-actin (red) were detected by immunofluorescence staining and confocal microscopy (scale bars, 10 μm). (B) Cells were treated with the indicated CamB concentrations for 24 h, and then lysed for the immunodetection of Snail. (C) Cells were treated with 30 μM CamB for 24 h, and then subjected to chromatin immunoprecipitation using anti-Snail antibody and RT-PCR using BMP4-specific primer, Input: total native chromatin, IgG: isotype control, NTC: no template control. (D) Cells were transfected with BMP4 promoter-vector and treated with the indicated CamB concentrations for 24 h, and then luciferase activity was analyzed by reporter assay. (E) Cells were transiently transfected with Snail-expressing vector and treated with 30 μM CamB for 24 h, and the binding of Snail to BMP4 promoter was determined by chromatin immunoprecipitation. (F) Cells were incubated with 30 μM CamB for 24h and lysed for mRNA extraction and qPCR analysis. (G, H) Cells were pretreated with MG132 or cytoheximide for 6 h, treated with 30 μM CamB for 24 h, and lysed for the immunodetection of Snail. (I) Cells were pretreated with MG132 for 6 h, treated with 30 μM CamB for 24 h, and lysed for immunoprecipitation by anti-Snail and immunoblotting by anti-ubiquitin and anti-Snail antibodies. Quantitative results were acquired by densitometric analysis and are presented as mean ± SD. * and **, $p < 0.01$ and $p < 0.001$ compared with control, respectively.*

4. Discussion

BMPs belong to the TGF-β superfamily, which were originally identified as osteo-inductive cytokines and have the effect of promoting bone and cartilage formation [14,15]. Recently, BMP4 plays critical roles in cancer progression and tumor metastasis via Smad signaling [16,17]. Our findings reveal that BMP4 stimuli remarkably enhance the cell adhesion, colony formation, cell motility, and invasion of CRC cells, and CamB co-treatment diminishes these BMP4-induced tumorigenicity. In

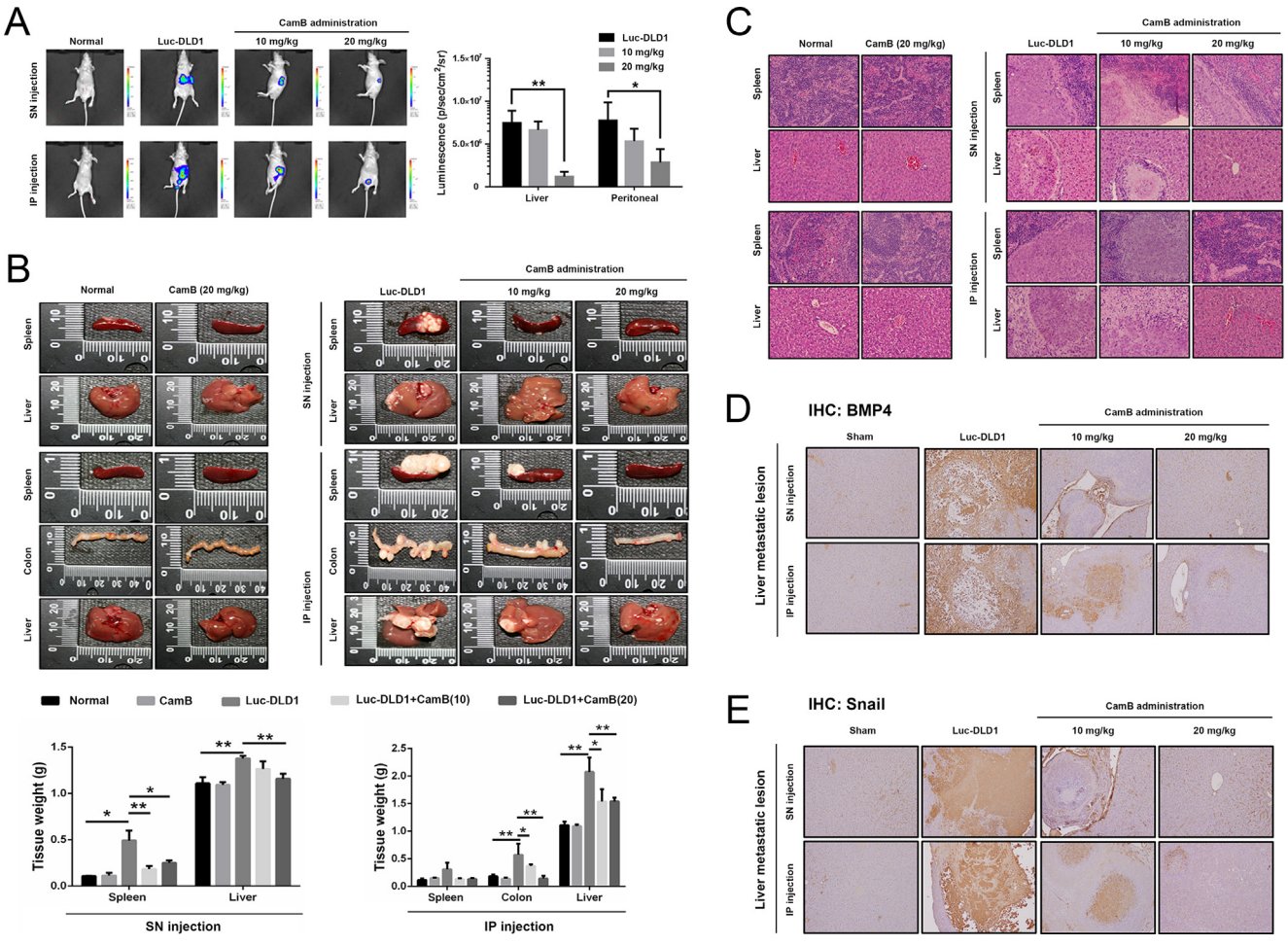

*Fig. 6. CamB administration in vivo inhibited CRC cell metastasis and reduced BMP4 and Snail expression in xenograft mice. Mice received Lu-DLD-1 cells via splenic or intraperitoneal injection, and then CamB (10 and 20 mg/kg) were orally administrated every 5 days. After 35 days of CamB administration, the mice were subjected to (A) Bioluminescent imaging analysis for luciferase activity and then sacrificed for the assessment of (B) metastatic lesion phenotype and tissue weights, (C) tumor metastasis by H&E staining, and (D, E) BMP4 and Snail level detection in liver metastatic lesion by IHC staining. Quantitative results are presented as mean ± SD. * and **, $p < 0.01$ and $p < 0.001$ compared with the control group, respectively.*

the canonical pathway, BMP4 binds to type I and II serine/threonine kinase receptors to form a complex, which triggers the phosphorylation of Smad1/5/9, and the phosphorylated Smad1/5/9 binds to Smad4 and translocates to the nucleus to exert gene regulation activity [18]. Our results show that CamB treatment decreased the phosphorylation of Smad1/5/9 and reduced nuclear Smad4 in DLD-1 cells. The results suggest that BMP4 plays an important role in promoting the metastatic capability of CRC cells and CamB can attenuate the metastatic capability of CRC cells via the inhibition of the BMP4/Smad cascade.

FAK signaling axis plays a pivotal role in controlling actin cytoskeleton remodeling, cell adhesion, and cell migration, which are involved in tumor metastasis [9,19]. In addition, FAK and BMP4-induced mesenchymal stem cell adipogenesis are linked together [20]. Interestingly, our observations showed that although the protein expression of the FAK axis, including FAK, talin, tensin 2, α-actinin, and vinculin, was not remarkably altered, CamB clearly suppressed the phosphorylation of FAK, Src, paxillin, and Akt. In addition, CamB also reduced the protein level and enzyme activity of small GTPases associated with FAK signaling, including Rho A, Cdc42, and Rac-1. In conclusion, these findings revealed that CamB treatment reduced BMP4 and its downstream signaling activation.

The induction of EMT is highly related to the progression and metastasis of CRC, and early and invasive metastasis is often the main cause of death in patients with CRC. Dynamic changes in cytoskeletal assembly during EMT leads to the loss of cell–cell contact and polarity in epithelial cells with enhanced cell motility. Thus, potent EMT inducers, such as Snail, Slug, and Twist, have been implicated in tumor progression and metastasis [21,22]. Our observations showed that Snail bound to the promotor of BMP4 and CamB clearly reduced Snail protein level and BMP4 transcription by increasing the ubiquitin-mediated degradation of Snail. Thus, CamB attenuates BMP4-induced metastatic potentials and inhibits the Snail-mediated EMT of CRC cells.

In conclusion, our findings demonstrated that CamB clearly attenuates the metastatic potential of CRC cells and inhibits the metastasis of CRC cells in xenograft mice through the suppression of BMP4-mediated Smad/FAK axis by promoting the ubiquitin-proteasome degradation of Snail. Collectively, the results suggest that CamB may be an effective adjuvant for CRC treatments, and BMP4 may be a potential molecular target for the development of anti-CRC drugs.

Funding statement

This work was supported by the Ministry of Science and Technology, Taiwan [grant no. MOST 108-2320-B-040-026-MY3, 107-2320-B-040-006-MY2 and 106-2320-B-040-017].

Conflict of interest

The authors declare no conflict of interest.

References

[1] Brenner H, Kloor M, Pox CP. Colorectal cancer. Lancet 2014; 383:1490–502.
[2] Nguyen LH, Goel A, Chung DC. Pathways of colorectal carcinogenesis. Gastroenterology 2020;158:291–302.
[3] Gupta GP, Massague J. Cancer metastasis: Building a framework. Cell 2006;127:679–95.
[4] Huang CF, Teng YH, Lu FJ, Hsu WH, Lin CL, Hung CC, et al. Beta-mangostin suppresses human hepatocellular carcinoma cell invasion through inhibition of MMP-2 and MMP-9 expression and activating the ERK and JNK pathways. Environ Toxicol 2017;32:2360–70.
[5] Lee M, Choi H, Kim KS, Kim DH, Kim CH, Lee YC. Curcumin downregulates human GM3 synthase (hST3Gal V) gene expression with autophagy induction in human colon carcinoma HCT116 cells. Evidence-based complementary and alternative medicine. eCAM 2018;2018:6746412.
[6] Park HJ, Choi YJ, Lee JH, Nam MJ. Naringenin causes ASK1-induced apoptosis via reactive oxygen species in human pancreatic cancer cells. Food Chem Toxicol 2017;99:1–8.
[7] Geethangili M, Tzeng YM. Review of pharmacological effects of antrodia camphorata and its bioactive compounds. Evidence-based complementary and alternative medicine. eCAM 2011;2011:212641.
[8] Lin WL, Lee YJ, Wang SM, Huang PY, Tseng TH. Inhibition of cell survival, cell cycle progression, tumor growth and cyclooxygenase-2 activity in MDA-MB-231 breast cancer cells by camphorataimide B. Eur J Pharmacol 2012;680:8–15.
[9] Huang CC, Hung CH, Hung TW, Lin YC, Wang CJ, Kao SH. Dietary delphinidin inhibits human colorectal cancer metastasis associating with upregulation of miR-204-3p and suppression of the integrin/FAK axis. Sci Rep 2019;9:18954.
[10] Wang WC, Tsai JJ, Kuo CY, Chen HM, Kao SH. Non-proteolytic house dust mite allergen, Der p 2, upregulated expression of tight junction molecule claudin-2 associated with Akt/GSK-3beta/beta-catenin signaling pathway. J Cell Biochem 2011;112:1544–51.
[11] Suryavanshi N, Ridley AJ. Determining Rho GTPase activity by an affinity-precipitation assay. Methods Mol Biol 2013; 1046:191–202.
[12] Lin CL, Ying TH, Yang SF, Wang SW, Cheng SP, Lee JJ, et al. Transcriptional suppression of miR-7 by MTA2 induces sp1-mediated KLK10 expression and metastasis of cervical cancer. Mol Ther Nucleic Acids 2020;20:699–710.
[13] Sugase T, Lam BQ, Danielson M, Terai M, Aplin AE, Gutkind JS, et al. Development and optimization of orthotopic liver metastasis xenograft mouse models in uveal melanoma. J Transl Med 2020;18:208–21.
[14] Briolay A, El Jamal A, Arnolfo P, Le Goff B, Blanchard F, Magne D, et al. Enhanced BMP-2/BMP-4 ratio in patients with peripheral spondyloarthritis and in cytokine- and stretch-stimulated mouse chondrocytes. Arthritis Res Ther 2020;22:234.
[15] Kaito T, Morimoto T, Mori Y, Kanayama S, Makino T, Takenaka S, et al. BMP-2/7 heterodimer strongly induces bone regeneration in the absence of increased soft tissue inflammation. Spine J 2018;18:139–46.

[16] Deng G, Chen Y, Guo C, Yin L, Han Y, Li Y, et al. BMP4 promotes the metastasis of gastric cancer by inducing epithelial-mesenchymal transition via ID1. J Cell Sci 2020: 133.
[17] Zhou Y, Liu Y, Zhang J, Yu D, Li A, Song H, et al. Autocrine BMP4 signaling enhances tumor aggressiveness via promoting wnt/beta-catenin signaling in IDH1-mutant gliomas. Transl Oncol 2020;13:125–34.
[18] Tsukamoto S, Mizuta T, Fujimoto M, Ohte S, Osawa K, Miyamoto A, et al. Smad9 is a new type of transcriptional regulator in bone morphogenetic protein signaling. Sci Rep 2014;4:7596.
[19] Bian ZQ, Luo Y, Guo F, Huang YZ, Zhong M, Cao H. Overexpressed ACP5 has prognostic value in colorectal cancer and promotes cell proliferation and tumorigenesis via FAK/PI3K/AKT signaling pathway. Am J Cancer Res 2019;9:22–35.
[20] Lee JS, Ha L, Kwon IK, Lim JY. The role of focal adhesion kinase in BMP4 induction of mesenchymal stem cell adipogenesis. Biochem Biophys Res Commun 2013;435:696–701.
[21] Gonzalez DM, Medici D. Signaling mechanisms of the epithelial-mesenchymal transition. Sci Signal 2014;7:re8.
[22] Lamouille S, Xu J, Derynck R. Molecular mechanisms of epithelial-mesenchymal transition. Nat Rev Mol Cell Biol 2014;15:178–96.